Turbulent Burning Rates of Gasoline Components, Part 1 - Effect of Fuel Structure of C$_6$ Hydrocarbons

A.A. Burluka[a], R.G. Gaughan[b], J.F. Griffiths[c], C. Mandilas[a,*], C.G.W. Sheppard[a], R. Woolley[d]

[a] School of Mechanical Engineering, The University of Leeds, Leeds LS2 9JT, UK

[b] ExxonMobil Research and Engineering Company, Paulsboro Technical Center, 600 Billingsport Road, Paulsboro, NJ 08066, United States

[c] School of Chemistry, University of Leeds, Leeds, LS2 9JT, United Kingdom

[d] The University of Sheffield, Department of Mechanical Engineering, Mappin Street, S1 3JD, UK

[*] Corresponding author. Present address: The Centre for Research and Technology, Hellas, Chemical Process & Energy Resources Institute, 3km Charilaou-Thermi Road, Thermi 57001, Greece

Abstract

Experimental measurements of turbulent burning velocities have been made of premixed hydrocarbon-air flames with six carbon atoms including unsaturated, cyclic and branched molecules. Measurements were performed at 0.5 MPa, 360 K and turbulent velocities of 2 and 6 m/s for a range of equivalence ratios. The laminar burning velocities were measured and used to interpret the turbulent data. The ranking of the laminar burning velocity was found to be 1-hexyne > 1-hexene > cyclohexane > n-hexane > 2-methyl pentane > 2,2 dimethyl butane for the range of equivalence rations tested. This ranking was found to be the same for the turbulent burning velocity measurements. As the turbulent velocity increased the relative differences between the fuels were found to increase (lean equivalence ratios), remain similar (around stoichiometric equivalence ratio), and decrease (rich equivalence ratios).

1. Introduction

Burning velocity has been the subject of numerous experimental and theoretical investigations spanning many decades, prompted to an extent by an interest in its effect on the performance of internal combustion engines. Burn rate affects engine performance, efficiency and cycle-to-cycle variability.

Thus, understanding the factors that influence the burn rate enables better control of engine combustion quality and emissions. The rate of combustion in an engine is a function of the turbulent burning velocity, which is itself a function of those physico-chemical features of a fuel-air mixture encapsulated in its laminar burning velocity, u_l, and the turbulence characteristics of the flow field within the engine. The influence of fuel structure on the laminar burning velocity has been reported [e.g. 1-5]. However, published data on the influence of hydrocarbon molecular structure on burn rate under turbulent conditions relevant to those in engine applications is virtually non-existent [6]. Consequently, the primary aim of the current work was to investigate the effects of fuel molecular structure and equivalence ratio, ϕ, on turbulent burning velocity of deflagrations.

Presented in this paper are experimentally determined turbulent and laminar burn rates for a set of hydrocarbons of varied structure, but all with 6 carbon atoms: 2,2-dimethyl butane, 2-methyl pentane n-hexane, cyclohexane, 1-hexene, cyclohexene and 1-hexyne. These fuels, with the exception of 1-hexyne, are representative components of automotive gasoline blends. Diagrams showing the molecular structures of the respective fuels are depicted in Figure 1.
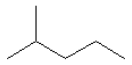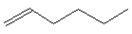
Fuel	Structure
2,2 dimethyl butane	
2, methyl pentane	
cyclohexane	
1-hexene	
cyclohexene	
1-hexyne	

Figure 1 – Schematic diagrams showing the molecular structure of the various fuels examined.

The turbulent burning velocity, u_t, is primarily a function of the turbulent velocity within the fluid. However it has long been acknowledged that fuel properties must also have an influence on u_t, as suggested by Damkholer whose expression for u_t included both the rms turbulent velocity, u' and the laminar burning velocity, u_l. Work performed in this study has focused on the influence of the fuel on u_t. The results are expressed in the form of the turbulent burning velocity plotted against ϕ. The effects on

burn rate of two different turbulent r.m.s. velocities were examined, $u' = 2$ and 6 m/s. These were chosen as they were thought to reflect realistic levels of turbulence found in industrial applications. Thus a further objective was to determine if relatively small differences in the fuel properties were relevant when u' is an order of magnitude greater than u_l. This is the first part of a two part study. In the second part turbulent burning velocities were obtained for straight chain alkanes from n-pentane to n-octane. For these fuels, chain structure is similar but there are differences in their chain length and molecular masses.

2. Experimental and Results Processing

The Leeds MkII spherical bomb operating under laminar and turbulent conditions, was employed for the studies. The effects on burn rate of two different turbulent r.m.s. velocities were examined ($u' = 2$ m/s and 6 m/s). Included below is a brief description of the experimental equipment and procedure; more detail is available in references [7-9]. All experiments incorporated schlieren-based imaging and pressure measurements to enable comparison of burn rate trends at both early and later stages of flame development. Although minor differences were evident, the general trends in burning velocity noted on the basis of schlieren and pressure based results were similar. Hence, for conciseness, the results reported here those based on the schlieren derived measurements.

A schematic diagram of the Data Acquisition System (DAQ) is shown in Figure 2. The light source was a 20 W tungsten element lamp. A convex lens was positioned at a distance equal to its focal length of 50 mm from the lamp. The light passing through this lens was focused at an iris, which was used to provide a single point light source. The expanding light beam was then focused into a parallel beam using a 150 mm plane convex lens (f-1000) and was passed through the combustion vessel window. On the other side of the vessel, another 150 mm convex plane lens (f-500) of focal length 500 mm was used to focus the light onto a pinhole of approximately 1 mm diameter. The light beam passing thought the pinhole was focused directly onto the camera chip. Centrally ignited advancing flames were imaged, to the window diameter of 150 mm, using a Photosonics Phantom Series 9 high speed digital camera with Complementary Metal Oxide Semiconductor (CMOS) chip. Laminar flames were recorded at 2000 frames/s. Turbulent flames were photographed at rates of 6300 and 9000 frames/s, for $u' = 2$ and 6 m/s, respectively.

Mixtures were prepared in the vessel. After each experiment the vessel was flushed several times with compressed air and evacuated. Dry cylinder air was provided for the combustible mixture. The calculated volumes of liquid fuels were injected into the vessel using a gas tight syringe. The fans were ran during mixture preparation, both to ensure full mixing and to assist heat transfer from the vessel's 2 kW electrical heater positioned close to a wall. For laminar studies the fans were switched off for a period of 60 seconds, following mixture preparation, before ignition. In turbulent tests the fans were maintained at the set speed, to produce the desired rms turbulence intensity throughout the mixture preparation, ignition and combustion period. The mixture temperature, prior to ignition, was measured using a K-type thermocouple situated inside the vessel.

Deflagrations were initiated at a nominal initial temperature of $T_i = 360$ K and pressure of $P_i = 0.5$ MPa, where published experimental data are relatively sparse, as most data available in the literature are for 0.1 MPa. The relatively high initial temperature ensured complete fuel vaporisation and contributed to the avoidance of condensation on the walls and windows after ignition, while the elevated initial pressure was adopted to provide conditions representative of combustion relevant to internal combustion engines. In the early stages of combustion, for flames of mean flame radius less than the window diameter, pressure and associated unburned gas temperature remained close to the initial values (since mixture volume fraction burned at that radius was less than 4%, with associated mass fraction burned less than 1%). Final bomb pressures were of the order $P_{comb} \approx 3.5$ MPa, (assuming a typical burned to unburned gas expansion ratio of $\rho_b / \rho_u \approx 7.0$). Experiments were conducted for a range of equivalence ratios, from lean ($\phi = 0.8$) to rich ($\phi = 1.6$).

At least two laminar and five turbulent deflagrations were performed at each condition. For laminar flames, the repeatability tolerance was set at a maximum of 2% in the time elapsed from ignition required to reach a pressure of 0.75 MPa for tests conducted on the same day; and 3% for tests conducted on different days. Turbulent tests exhibited inherent cyclic variability and thus a similar tolerance approach could not be followed; typical experimental scatter for turbulent flames was circa 10% (in coefficient of variance, COV), independent of the r.m.s. turbulent velocity.
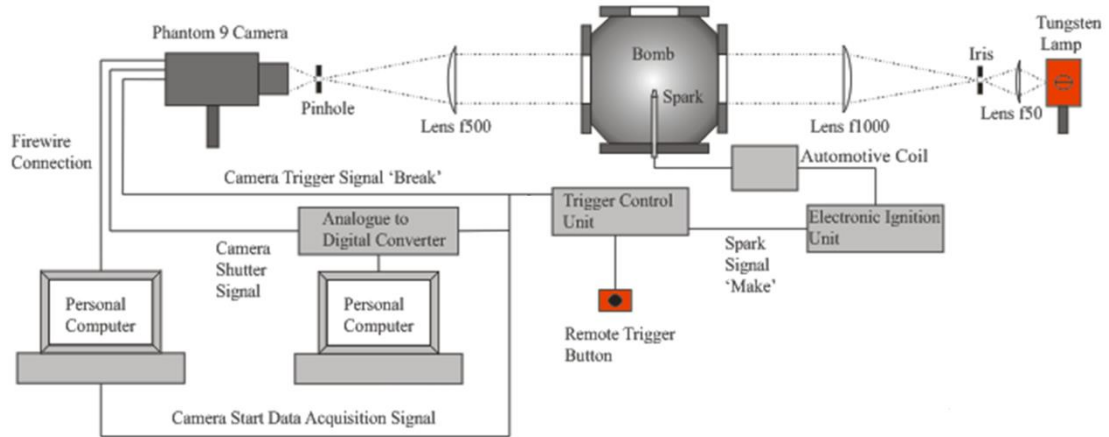
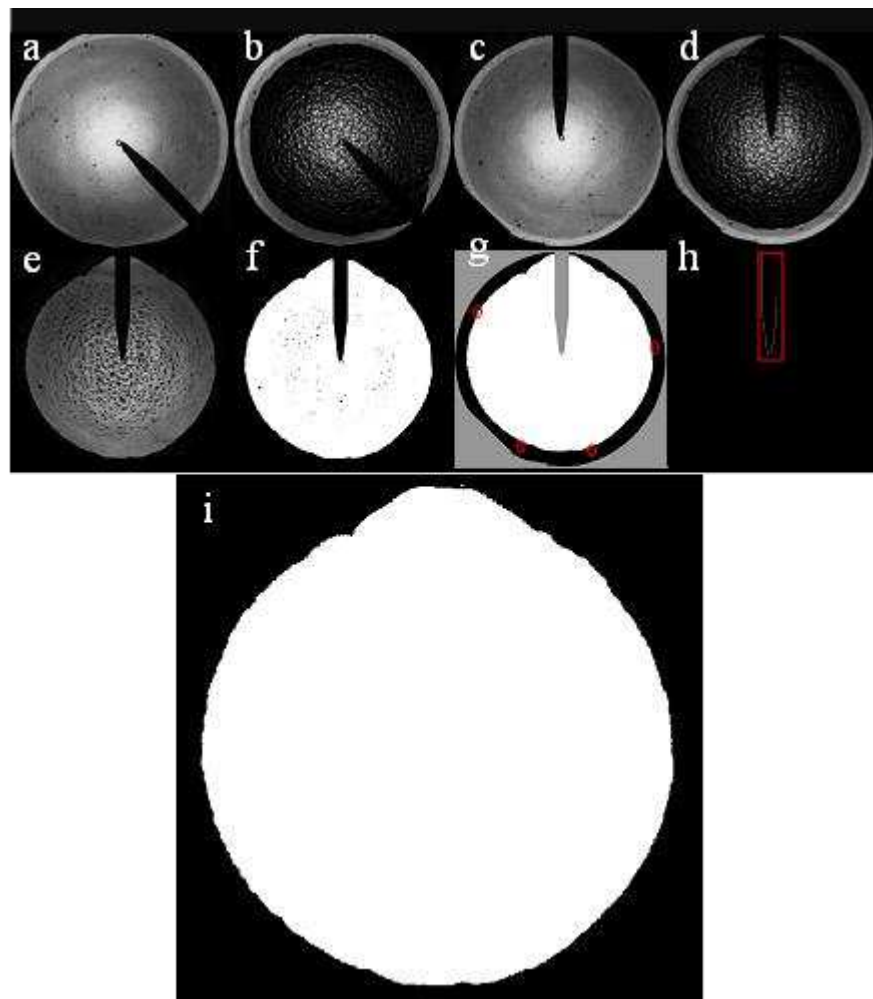Figure 2 – Schematic of the DAQ for schlieren imaging of deflagrations inside the bomb.

Figure 3 – Processing steps for a sample n-octane laminar stoichiometric flame.

The laminar burning velocity was obtained using what has become a typical method of its determination from spherically expanding flames. Image processing was applied to identify the burned gas area; assuming a spherical flame, the projected flame area, A, was readily determined by converting the schlieren images into binary black (unburned) and white (burned) regions. Image binarisation was achieved via a series of custom built MATLAB scripts. The main processing steps involved during image manipulation are highlighted in Figure 3. Initially all original images (a, b) of a flame movie were rotated to transfer the spark plug probe to the top (c, d). Next, the pre-ignition image was subtracted from the current flame image (e). The subtracted image was then binarised (f) before combining it to the pre-ignition grayed image. The combined image (g) was then used to attain the edges of the spark plug probe protruding into the flame (h). The final step involved filtering of the noise around the flame image (white pixels circled in red in image g) and removal of the spark plug probe from the flame to acquire the finalised image (i) which was used for the determination of the flame area.

The schlieren edge has been shown to represent an isotherm of approximately 305 K and the cold front flame radius, r_u, related to radius r_{sch} by:

$$r_u = r_{sch} + 1.95\delta_l \left(\frac{\rho_u}{\rho_b}\right)^{0.5} \tag{1}$$

Here, ρ_u is the density of the reactants, ρ_b is the density of the products and δ_l is the laminar flame thickness. The laminar flame thickness was defined as,

$$\delta_l = \frac{v}{u_l} \tag{2}$$

where u_l is the stretch-free burning velocity and v is the kinematic viscosity of the reactants. The flame speed, S_n, was found by differentiating cold front flame radius with time,

$$S_n = \frac{dr_u}{dt} \tag{3}$$

The stretch rate of the flame determined using,

$$a = \frac{1}{A}\frac{dA}{dt} = \frac{1}{4\pi r_u^2}\frac{d(4\pi r_u^2)}{dt} = \frac{2}{r_u}S_n \tag{4}$$

As flame radius increases, the total stretch rate approaches zero so that $S_n \rightarrow S_s$, $u_n \rightarrow u_l$. Therefore, the stretch-free terms can be given by the values of the corresponding stretched terms in its linear form,

$$S_s - S_n = L_b \, \alpha \qquad\qquad (5)$$

The burnt Markstein length, L_b, is the slope and the stretch-free flame speed, S_s, is the y-axis intercept. The Markstein length (L_b) of a flame is a physico-chemical flame parameter, customarily used to characterise the effect of stretch rate on flame speed [10]. High positive values of L_b indicate that as the flame expands, and becomes increasingly less stretched, there is a gain in flame speed; the opposite is true for flames with negative Markstein length values. Applying mass conservation, the stretch-free burning velocity can be related to S_s by

$$u_l = S_s \frac{\rho_b}{\rho_u} \qquad\qquad (6)$$

A non linear variation of flame speed with stretch has also been derived [11],

$$\left(\frac{S_n}{S_s}\right)^2 \ln\left(\left(\frac{S_n}{S_s}\right)^2\right) = \frac{2L_b\alpha}{S_s} \qquad\qquad (7)$$

This was compared to the linear results given in Eq. 5.

It is important to note that Equations 6 and 7 were applied only when there was sufficient data at appropriate conditions to perform the fit described. In many cases, especially for fuels at $\phi > 1.2$, cellularity occurred too early to allow for such a fit. In such cases laminar burn rate was determined using,

$$u_l = u_{n,\min} \qquad\qquad (8)$$

The approach followed for determination of the mean flame radius of turbulent flames is similar to that described above for laminar flames. The definition of the turbulent burning velocity used here is given below.

3. Results and Discussion

3.1 Laminar Burning Velocity

Laminar burning velocity (u_l) results for the fuels are displayed in Figure 4. Solid lines refer to results obtained by extrapolating the measured flame speeds to zero stretch then dividing the flame speed by the density ratio [12]. Dotted lines correspond to u_l values computed using $u_l = u_{n,\min}$, where, u_n is the stretched entrainment burning velocity. All rich flames for the fuels examined showed signs of cellularity as early as a mean flame radius of 10-15 mm. Consequently, too few data points were

available to determine L_b. Burning velocities obtained in this way cannot be considered to be rigorously defined but represent a pragmatic approach to obtaining laminar burning velocity data to aid the analysis of subsequent turbulent burning measurements.
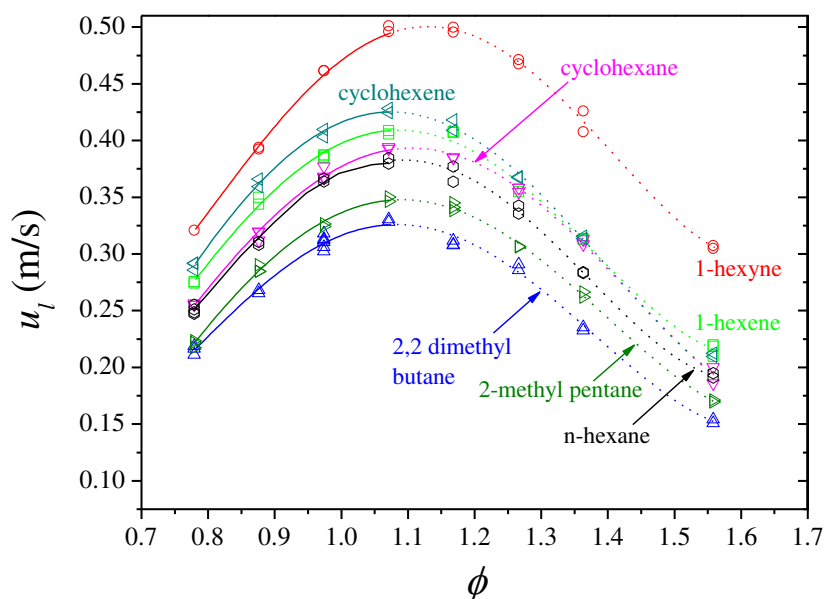

Figure 4 – Plots of stretch-free burning velocities against ϕ. Obtained using Eq. 7.

The u_l peaked close to $\phi = 1.1$ and demonstrated a dependence on molecular structure that was similar at all ϕ explored. Overlaps in u_l ranking were evident only in the richest mixtures, where the impact of cellularity is greatest and uncertainty in error in u_l the largest.

The unsaturated fuels 1-hexyne (triple C≡C bond) and cyclohexene (double C=C and ring structure) had the highest u_l. Ranking of the remaining fuels was: 1-hexene (unsaturated, double C=C bond), cyclohexane (unsaturated, ring structure) and n-hexane (saturated). The iso-alkanes burned slowest, with the double branched 2,2 dimethyl butane being noticeably slower than the single branched 2-methyl pentane.

The Markstein length (L_b) of a flame is a physico-chemical flame parameter, customarily used to characterise the effect of stretch rate on flame speed [10]. Its values are shown in Figure 5. Although of notable scatter, with COV as high as 25% [13], differences in the L_b measured for the fuels (at fixed ϕ) were small, with the overall trend being a decrease in L_b with ϕ. Nevertheless, L_b values remained positive at all ϕ for which Markstein lengths could be experimentally measured. This similarity in L_b for the various fuels can be attributed to their comparable thermo-diffusive characteristics, arising from their similar molar mass.
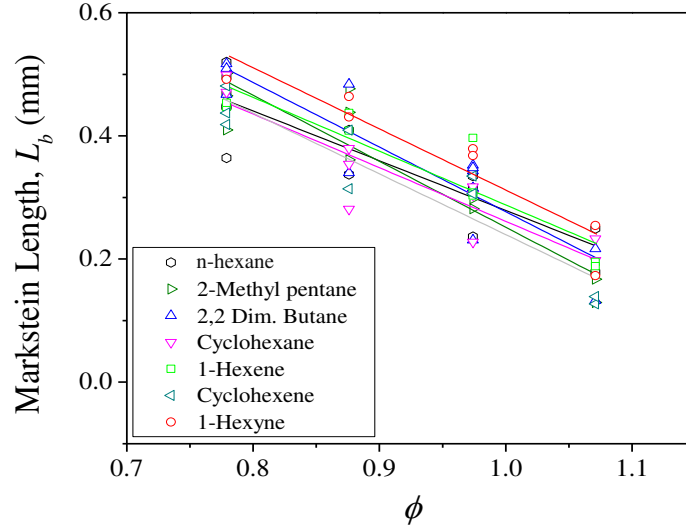
Figure 5 – Measured burnt Markstein lengths, L_b. Obtained using Eq. 7.

The experimentally measured values of u_l obtained here, for n-hexane and cyclohexane, were compared with Chemkin Premix code [14] at the same unburned temperature and pressure. Multi-component formulation for transport properties including Soret diffusion were used. The JetSurF 2.0 mechanism [15] was selected as it has been previously compared with laminar burning measurements [5] at elevated conditions and it was possible to compare a number of the fuels with a single mechanism. The comparisons are shown in Figure 6. The agreement between the experiments and model at lean ϕ is good. Beyond $\phi = 1$ the flames were cellular from ignition so the experimental data corresponds to the minimum burning velocity recorded. It is to be expected that cellularity increases the burn rate so it might be presumed that the measured values are higher than the computed values. The comparison is to some extent meaningless as the flames do not exist as a single uninterrupted flame front under these conditions as thermo diffusive effects would result in localized quenching of the flame surface [10]. However, the computed u_l could provide a useful, unambiguously defined reference although they cannot be experimentally verified.
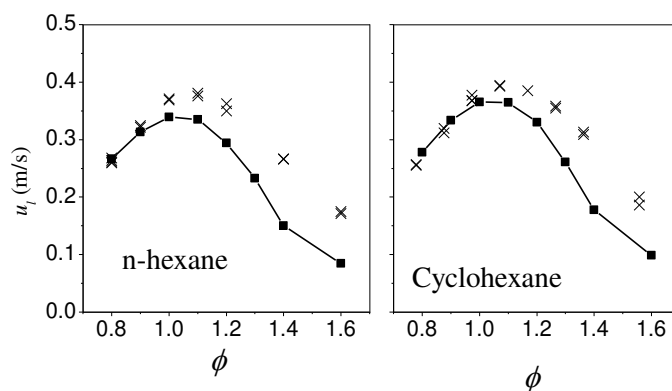
Figure 6 – Comparison of experimental burning velocity (crosses) with numerical computations (filled squares) performed with Jetsurf 2.0. Initial temperature and pressure 360 K and 0.5 MPa.

The development of hydrocarbon kinetic mechanisms has occurred rapidly in the previous few decades and this, allied with improvements in u_l experimental methods has resulted in better understanding of the key combustion processes taking place within the flame. Using the suggestions of previous workers [4-5, 16-19] reasons for the differences in u_l are given below:

1. Unsaturated hydrocarbons have higher burning velocities than saturated hydrocarbons. It is implicit that a lower proportion of H atoms available in the "radical pool" formed during oxidation leads to a weaker propensity for chain branching reactions to boost burn rate [4, 17]. Hydrogen atoms are more easily abstracted from unsaturated molecules (i.e. 1-hexyne, 1-hexene, cyclohexene) due to the presence of the relatively weaker allylic C-H bond; this promotes an additional, kinetic, advantage to the effect of their higher T_{ad}. There is also a larger number of the combustion routes for the break-down of alkenes/alkynes via ethyl radicals, producing extremely fast burning intermediate species, such as ethylene, vinyl radical and acetylene [4].

2. Branched alkanes burn slower than their straight chain equivalent. Combustion of the branched alkanes (i.e. 2,2 dimethyl butane and 2-methyl pentane) produces more, relatively non-reactive CH_3 radicals, compared to n-hexane oxidation, which contributes to a reduction in the overall burn rate [4, 16]. The lower u_l of the branched alkanes can also be related to the propensity of hydrogen abstraction during oxidation. For example, in the case of 2,2 dimethyl butane, four out of the six carbon atoms constitute methyl radicals with strong C-H bonds (ΔH^o ~430 kJ/mol);

with only two methylene groups, possessing rather weaker C-H bonds (ΔH^o ~405 kJ/mol). However, 2-methyl pentane contains only three methyl groups and, consequently, 3 methylene groups and consequently has a slightly higher burning velocity than 2,2 dimethyl butane.

3.2 Turbulent Burning Velocity

Contours of successive flame edges generated from schlieren images of lean and rich turbulent n-octane-air flames ($\phi = 0.8$ and 1.2) are presented in Figure 7. As noted by previous workers there are observable differences in way in which flames of different ϕ propagate [20]. The lean flames, $\phi = 0.8$, can be seen to be distorted by the turbulent flow field (i.e. local protrusions and recesses). This is in distinct contrast to the development of $\phi = 1.2$ flames which propagated outwards in a more uniform manner.
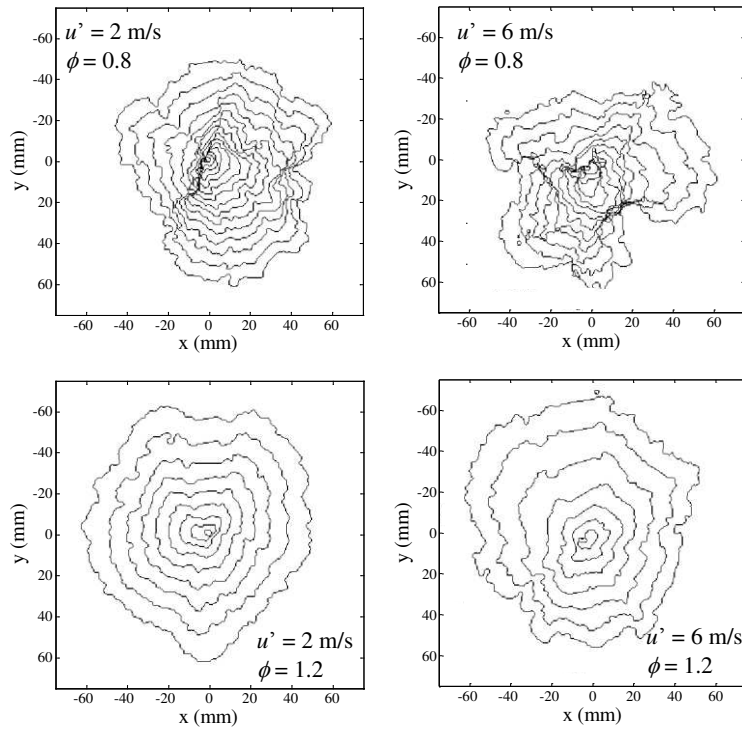

Figure 7 – Sample flame contours of turbulent flames.

Experimental turbulent burning velocities, $u_{te,}$ derived from the schlieren films are plotted against flame radius and shown in Figure 8, for n-octane/air mixtures at $\phi = 1.0$. Turbulent flames continuously accelerate from ignition. This is explained as 'turbulent flame development', when the flame kernel is

small only a proportion of the turbulent eddies (those smaller than the flame) can wrinkle the flame, increasing its surface area and hence its burning velocity [21]. As the flame grows more eddies are able to wrinkle the flame and it accelerates, the flame brush thickness has also been shown to increase with flame radius [22].
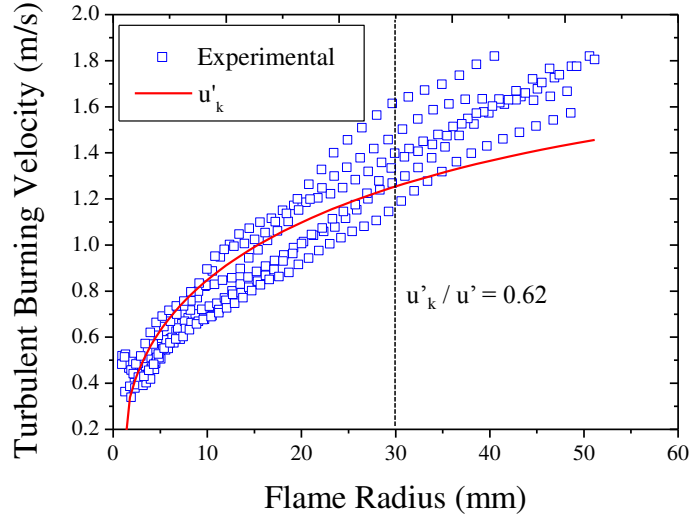

Figure 8 – An example turbulent flame growth versus flame radius under at $u' = 2$ m/s n-octane-air mixtures at $\phi = 1.0$. The effective r.m.s turbulent velocity, u'_k is also shown.

The primary object of this work is to compare the relative propagation rate of different fuels and fuel + air mixtures. Turbulent flames growing in a closed volume accelerate [23-26], with the rate of acceleration being a function of turbulence [27] and to a lesser extent laminar flame speed [28]. In order to achieve a consistent comparison it is necessary to define the burning velocity and an appropriate reference point.

1. *The burning velocity.* The entrainment turbulent velocity, u_{te} has been adopted. A mean flame radius, r_{sch}, is used based on A_{sch}, and the turbulent flame speed is given by

$$S_{te} = \frac{dr_{sch}}{dt} \tag{9}$$

Here, the subscript "e" denotes that the flame speed is based on an entrainment of unburned gas. The burning velocity can then be determined by accounting for the expansion of the burned gas,

$$u_{te} = \frac{\rho_b}{\rho_u}\frac{dr_{sch}}{dt} = \frac{\rho_b}{\rho_u}S_{te} \tag{10}$$

This definition of turbulent burning velocity derived from schlieren measurements has been compared with other definitions obtained using pressure transducers and laser sheet measurements [24, 29]. With suitable post processing it is possible to obtain alternatively defined burning velocities however this is avoided here as it not the objective of the work and runs the risk of propagating errors.

2. *The burning velocity was compared at a radius*, r_{sch} = 30mm. This radius was selected to be sufficiently large to ensure that there was no residual consequence of the initiation spark energy [27]. The comparison of turbulent burning velocities at a fixed size may result in uncertainties as the selected radius was not attained at the same dimensionless time (e.g. time from ignition / integral time scale). As the turbulent properties (*u'* and *L*) are fixed for comparison differences in time taken for flames to propagate across the vessel arise from different u_l and in particular ρ_b/ρ_u. At a flame radius of r_{sch} = 30 mm, each flame would have experienced more than one integral length scale (*L* = 20 mm [30]) and it would not have interacted with the fans. Following an approach used by previous workers [31] an effective r.m.s turbulent velocity, u'_k can be found by integrating the turbulent power spectrum density and used to characterize turbulent flame development (the observed continuous increase in burn rate from ignition). For u'_k/u' = 1 the flame encompasses all magnitudes of turbulent eddies. At r_{sch} = 30 mm u'_k/u' was determined to be ~62% [31] thus an appreciably proportion of the turbulent flow field has interacted with the flame. It has been shown that ranking fuels with respect to u_{te} at r_{sch} = 30mm is representative of their ranking at any other radii for 30 mm < r_{sch} < 65 mm [13]. Hence, trends with fuel type at r_{sch} = 30 mm may be considered representative of the behaviour of the different flames.

Turbulent burn rate results at *u'* = 2 and 6 m/s are shown in Figure 9. The curves are 3rd order polynomial fits to the experimental data. The experimental scatter in u_{te} was ~10% COV and proved independent of *u'*. This was in accord with previous measurements in this vessel [21]. Turbulence significantly enhanced the burn rate of all the fuels. The results set out in Figure 9 suggest that the influence of fuel molecular structure noted for laminar flames carries over to turbulent flames. The fuels 2,2 dimethyl butane and 1-hexyne remained the slowest and fastest fuels respectively. In order to examine the relative differences between the fuels, results have been plotted with reference to the burning velocity of n-hexane in Figure 10.
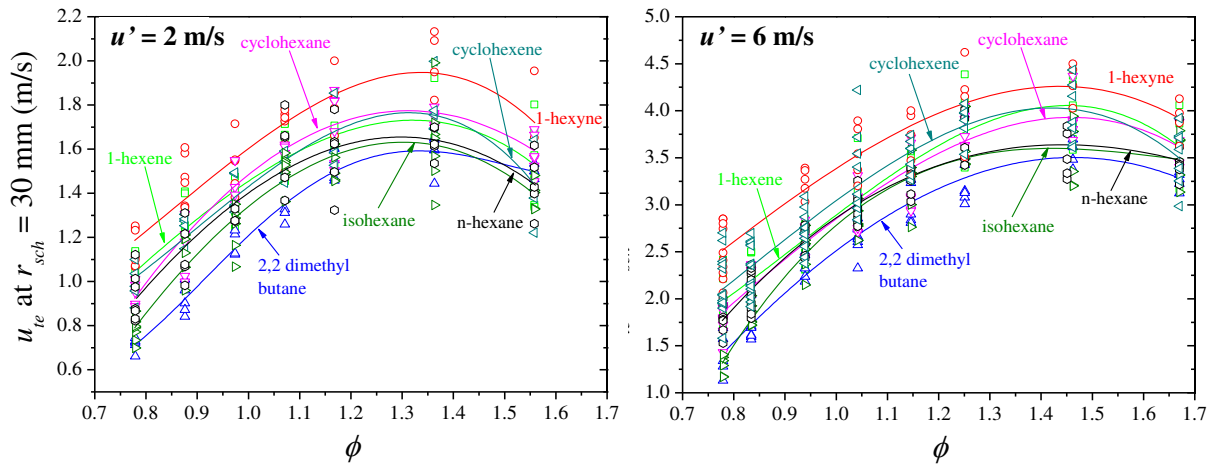
Figure 9 – Entrainment turbulent burning velocities at mean flame radii of 30 mm, plotted against ϕ.

At both turbulent intensities, the turbulent burning velocities followed the same qualitative trends as for u_l. However, 1-hexyne was the fastest burning of all the fuels under laminar conditions (e.g., 30-50% faster than n-hexane) whereas, under turbulent conditions, 1-hexyne was typically only 20% faster than n-hexane. Cyclohexene, cyclohexene and 1-hexene, typically, burned 10% faster than n-hexane irrespective of whether the unburned mixture was laminar or turbulent. Iso-hexane and 2,2 dimethylbutane were up to 10% slower than n-hexane for both laminar and turbulent conditions. At the extreme lean condition tested ($\phi = 0.78$) the difference between the fastest fuel (1-hexyne) and slowest fuels (iso-hexane and 2,2 dimethylbutane) was found to increase with u'. In contrast, at the other ϕ, the relative differences between the fuels decreased as u' increased indicating that the magnitude of u_l became less influential, particularly at rich ϕ.
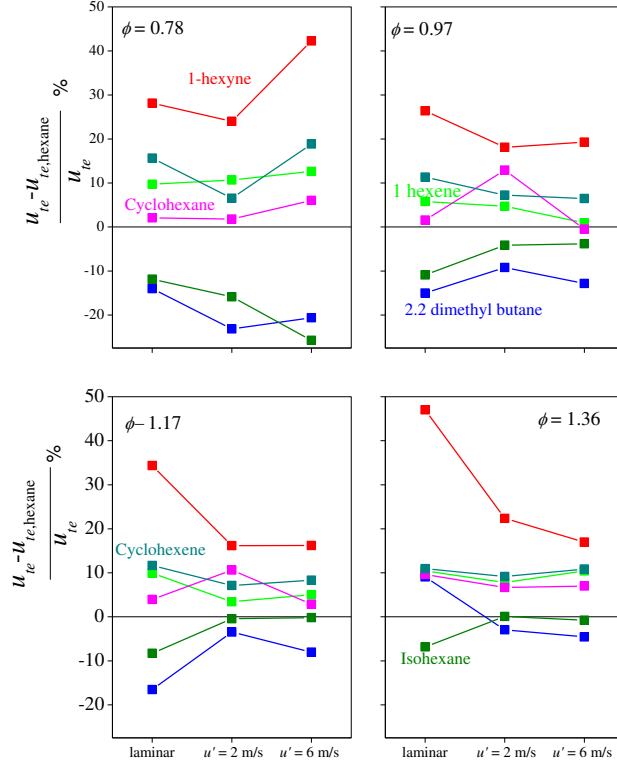
Figure 10 – Relative differences in turbulent burning velocity. Fuels referenced against n-hexane. Averaged values used.

Laminar flamelets have been observed up to high levels of turbulence. In his review Driscoll [32] suggested that there was experimental evidence for the existence of flamelets for Karlovitz Numbers exceeding 10. Here, the Karlovitz number was defined as:

$$Ka = \left(\frac{u'}{u_l}\right)^{3/2} \left(\frac{u_l L}{\alpha_0}\right)^{-1/2} \left(\frac{(T_p + T_R)/2}{300K}\right)^{1/2} \qquad (11)$$

Where α_0 is the diffusivity of nitrogen at 300 K, which is equal to 0.15 cm^2/s, and T_P and T_R are the temperatures of the reactants and products. In this study Ka varied between 1 and 4 for $u' =2$ m/s and 5 and 20 for $u' = 6$ m/s. Thickening of the preheat zone has been observed for lean propane flames, this has been attributed to response of the flame to the net strain rate within the fluid [32], therefore, the flames studied here at lean equivalence ratios may be experiencing broadening on the preheat zone. This impacts on the flames to different degrees; for example, the unsaturated molecules in which hydrogen atoms are more easily abstracted were measured to be less affected than the branched ones. For rich equivalence ratios (for hydrocarbon fuels heavier than propane) thermodiffusive effects have been

demonstrated, resulting in flamelet thickening and localized extinction in areas of negative curvature. At these rich equivalence ratio the relative differences between the molecules seems to decrease; perhaps the diffusion processes that depend on the mass of the molecule become more important.

There are a number of simple expressions for turbulent burning velocity that are used as sub-models in more complex models that are able to represent the combustion chamber geometry. An example is the Zimont model which is included in FLUENT. Some of these expressions use a power law format where each of the significant parameters are expressed in the form $u_t = f(u_l{}^a, u'{}^b, ...)$. Using the results presented here the effect of modifying u_l on u_{te} can be tested whilst all other parameters are constant i.e. u', L_b, L.

Shown in Figure 11 are values of u_{te} log plotted against u_l. The data are sub-divided into groups of constant u' and ϕ and contain information for each of the fuels tested. Linear fits are shown for each group and represent fits of the form $u_{te} \propto u_l{}^n$. There appears to be a strong influence of the equivalence ratio. At the leanest ϕ values of u_{te} noticeably increased with u_l. For the richest mixtures the impact changes in u_l had a lesser impact on u_{te}.
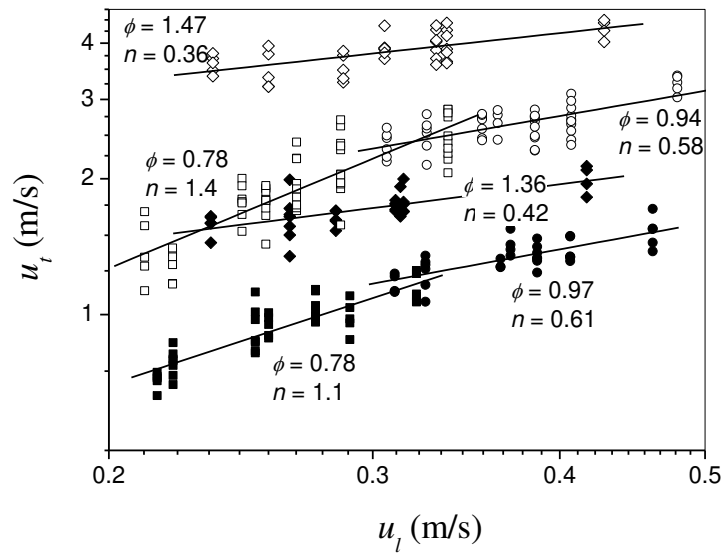

Figure 11. Values of u_t plotted against u_l. Filled symbols, $u' = 2$ m/s; open symbols, $u' = 6$ m/s. Each group is made up of data from different fuels at the same u' and ϕ. The gradients of the fits shown given as n.

Plotted in Figure 12 are values of n against ϕ for both u' examined. The magnitude of n is largest at leanest equivalence ratios and decreases as the mixture becomes leaner. For $\phi = 1.1$ and the difference the fastest fuel richer mixtures n could be considered to be constant or decreasing with increasing ϕ although at a slower rate. These values resemble the trends observed in L_b. Thus the turbulent burning velocity of leanest stretch sensitive flames are most sensitive to changes in the laminar burning velocity. Rich thermo-diffusively unstable flames are relatively less sensitive to changes in u_l associated with different fuels.
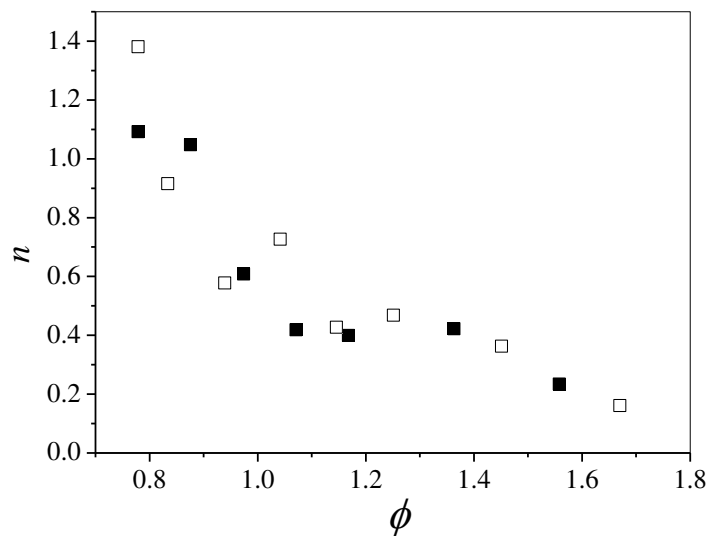

Figure 12. Values of the exponent, n where $u_{te} \propto u_l^n$. Filled symbols, $u' = 2$ m/s; open symbols, $u' = 6$ m/s.

4. Conclusions

The turbulent burning velocity remains a relatively poorly quantified parameter. The competing influence of the flame and flow field properties results in variation in experimental and modelled measurements. The result is that the impact of changing the fuel on the turbulent burning velocity cannot be predicted with certainty. Here the velocity of premixed turbulent flames of hydrocarbon molecules consisting of six carbon atoms have been measured in a spherical fan stirred combustion vessel. Tests have been performed for a range of equivalence rations and two turbulent velocities, $u' = 2$ and 6 m/s. In order to aid interpretation of the turbulent results the laminar burning velocity was also determined from filming of spherical expanding flames within the same vessel. The results are expressed in the form

of the turbulent burning velocity plotted against ϕ at a mean flame radius of 30 mm. This approach builds on previous studies [21, 33] where it was found to be successful at illuminating the differences between fuels, which tend to be most marked at rich and lean ϕ.

- The unsaturated fuels 1-hexyne (triple C≡C bond) and cyclohexene (double C=C and ring structure) had the highest u_l. Ranking of the remaining fuels was: 1-hexene (unsaturated, double C=C bond), cyclohexane (unsaturated, ring structure) and n-hexane (saturated). The iso-alkanes burned slowest, with the double branched 2,2 dimethyl butane noticeably slower than the single branched 2-methyl pentane. This is in agreement with previous studies.

- The measurements of Markstein Length, L_b, were highly scattered. However, no significant differences in L_b were observed. This similarity in L_b for the various fuels can be attributed to their similar thermo-diffusive characteristics, arising from their close molar mass.

- At both turbulent intensities, the turbulent burning velocities followed the same qualitative trends and rankings as for u_l.

- At $\phi = 0.78$ the difference between the fastest fuel, hexyne, and slowest fuels ,iso-hexane and 2,2 dimethylbutane, appeared to increase with u'. In contrast at the other ϕ the relative differences between the fuels decreased as u' increased indicating that the magnitude of u_l becomes less influential, particularly at rich ϕ.

- The turbulent burning velocity of leanest stretch sensitive flames are most sensitive to changes in the laminar burning velocity. Rich thermo-diffusively unstable flames are relatively less sensitive to changes in u_l associated with different fuels.

Acknowledgements

References

1. Gerstein, M., Levine, O., Wong, E.L., J Am Chem Soc 73 (1951) 418

2. Davis, S.G., Law, C.K., Combust Sci Technol 140 (1998) 427

3. Vagelopoulos, C.M., Egolfopoulos, F.N., P Combust Inst 27 (1998) 513

4. Farrell, J.T., Johnston, R.J., Androulakis, I.P., SAE Tech Paper (2004) 2004-01-2936

5. Wu, F., Kelley, A.P., Law, C.K., Combust Flame 159 (2012) 1417

6. A.A. Burluka, R.G. Gaughan, J.F. Griffiths, C. Mandilas, C.G.W. Sheppard, R. Woolley, 7th European Combustion Meeting, Budapest, 2015

7. Gillespie, L., Lawes, M., Sheppard, C.G.W., Woolley, R., SAE Tech Paper (2000) 2000-01-0192

8. Bradley, D., Gaskel, P.H., Gu, X.J., Combust Flame 104 (1996) 176

9. Bradley, D., Hicks, R.A., Lawes, M., Sheppard, C.G.W., Woolley, R., Combust Flame 115 (1998) 126

10. Bradley, D., Sheppard, C.G.W., Woolley, R., Greenhalgh, D.A., Lockett, R.D., Combust Flame 122 (2000) 195

11. A.P. Kelley, A.J. Smallbone, D.L. Zhu, C.K. Law, Proceedings of the Combustion Institute 33 (2011) 963–970

12. Kitagawa, T., Nakahara, T., Maruyana, K., Kado, K., Hayakawa, A., Kobyashi, S., Int J Hydrogen Energ 33 (2008) 5842

13. Mandilas, C., "Laminar and turbulent burning characteristics of hydrocarbon fuels", PhD Thesis, University of Leeds, 2008

14. Kee, R.J., Grcar, J.F., Smooke, M.D., Miller, J.A., A FORTRAN Program for Modeling Steady Laminar One-dimensional Premixed Flames, Sandia Report, SAND85, 8240, Sandia National Laboratories, 1985

15. H. Wang, E. Dames, B. Sirjean, D.A. Sheen, R. Tangko, A. Violi, et al., A High temperature Chemical Kinetic Model of n-Alkane (up to n-Dodecane),Cyclohexane, and Methyl-, Ethyl-, n-Propyl and n-Butyl-Cyclohexane Oxidation at High Temperatures, University of Southern California, 2010

16. Dryer, F.L., Westbrook, C.K., Prog Energ Combust 10 (1984) 1

17. Johnston, R.J., Farrell, J.T., P Combust Inst 30 (2005) 217

18. Gaughan, R., Private Communication, 2007

19. Turns, S., An Introduction to Combustion, Concepts and Applications, 2nd Edition, McGraw Hill, 2000

20. Lawes, M., Ormsby, M.P., Sheppard, C.G.W., Woolley R., Combust Flame, 159 (2012) 1949

21. Ormsby, M.P., Turbulent Flame Development in a High-Pressure Combustion Vessel, University of Leeds, 2005, Thesis

22. Burluka, A.A., Hussin, A.M.T.E., Sheppard, C.G.W., Liu, K., Sanderson, V., Flow Turbul Combust 86 (2011) 735

23. Lawes, M., Ormsby, M.P., Sheppard, C.G.W., Woolley, R., Combust Sci Technol 177 (2005) 127

24. Lipatnikov A.N., Chomiak J., Combust Sci Technol 137 (1998) 277

25. Borghi, R., Prog Energ Combust 14 (1988) 245

26. Zimont, V.L., Exp Therm Fluid Sci 21 (2000) 179

27. Bradley, D., Lung, F.K., Combust Flame 69 (1987) 71

28. Bradley, D., Haq, M.Z., Hicks R.A., Kitagawa T., Lawes M., Sheppard, C.G.W. and Woolley R., Combust Flame 133 (2003) 415

29. Lamourex, N., Djebaili-Chaumeix, N., Paillard, C.E., 2nd Mediterranean Comb Symp, Exp Therm Fluid Sci 27 (2003) 385

30. Nwagwe, K., Weller, H.G., Tabor, G.R., Gosman, A.D., Lawes, M., Sheppard, C.G.W., Woolley, R., P Combust Inst 28 (2000) 51

31. Abdel-Gayed, R.G., Bradley, D., Lawes, M., Proc R Soc Lond A414 (1987) 389

32. Driscoll, J.F., Prog Energ Combust Sci 34 (2008) 91

33. Mandilas, C. Ormsby, M.P., Sheppard, C.G.W., Woolley, R., Proc Comb Inst 31 (2007) 1443